MATHEMATICAL BIOSCIENCES
AND ENGINEERING
Volume **9**, Number **2**, April **2012**

doi:10.3934/mbe.2012.9.215

pp. **215–239**

# LONGTIME BEHAVIOR OF ONE-DIMENSIONAL BIOFILM MODELS WITH SHEAR DEPENDENT DETACHMENT RATES

Fazal Abbas, Rangarajan Sudarsan and Hermann J. Eberl

Dept. Mathematics and Statistics, University of Guelph
50 Stone Rd E, Guelph, ON, N1G 2W1, Canada

(Communicated by Hal Smith)

Abstract. We investigate the role of non shear stress and shear stressed based detachment rate functions for the longterm behavior of one-dimensional biofilm models. We find that the particular choice of a detachment rate function can affect the model prediction of persistence or washout of the biofilm. Moreover, by comparing biofilms in three settings: (i) Couette flow reactors, (ii) Poiseuille flow with fixed flow rate and (iii) Poiseuille flow with fixed pressure drop, we find that not only the bulk flow Reynolds number but also the particular mechanism driving the flow can play a crucial role for longterm behavior. We treat primarily the single species-case that can be analyzed with elementary ODE techniques. But we show also how the results, to some extent, can be carried over to multi-species biofilm models, and to biofilm models that are embedded in reactor mass balances.

1. **Introduction.** Bacterial biofilms are microbial depositions on biotic or abiotic immersed surfaces. Bacteria attach to the surface (called substratum in the biofilm literature) and start producing gluey extracellular polymeric substances (EPS), in which they are themselves embedded [14, 36]. This EPS matrix offers the cells protection against harmful external stimuli.

Biofilm based technologies have been developed in Environmental Engineering for many decades, originally in wastewater treatment, more recently also for soil remediation and groundwater protection. Other occurrences of biofilms are considered negative. For example, in industrial equipment biofilms can lead to microbially induced corrosion (biocorrosion) or to biofouling that reduces performance efficiency. In food processing equipment they lead to hygienic risk. In a medical context, biofilms can lead to infections that are essentially more difficult to treat with antibiotics than bacterial infections caused by planktonic bacteria.

Biofilms are spatially structured microbial populations. Substrates that are necessary to sustain microbial growth, such as nutrients or oxygen (in the aerobic case) diffuse through the biofilm matrix, in most cases from the aqueous bulk phase. They are consumed and depleted by the bacteria as they diffuse through the biofilm. This leads to substrate gradients. Consequently, bacteria in the inner layers of a biofilm experience different living conditions than bacteria in the outer layers, leading to variations of metabolic activity, and in some cases to the establishment of micro environments, e.g., such as anaerobic niches in otherwise aerobic communities.

2000 *Mathematics Subject Classification.* Primary: 92D25; Secondary: 34C60.
*Key words and phrases.* Mathematical model, biofilm, detachment.

Biofilms grow in diverse hydrodynamic conditions – from creeping flow in capillaries to turbulent flow in pipes. They experience shear forces which can disrupt the mechanical stability of the biofilm causing them to erode. This phenomenon is generally referred to as biofilm detachment and has been described in many experiments as a main mechanism to balance growth, allowing the biofilm to reach a steady state. In some industrial systems, detaching biomass is washed out, in other applications in enters the production stream. For example, a listeriosis outbreak in Canada in 2008 that cost 20 lives was related to detachment of a *Listeria monocytogenes* biofilm from a meat processing equipment. In other industrial systems, not detaching biofilms can affect performance. A phenomenon related to detachment is bioclogging, usually of porous media. This refers to biofilms that clog the pore space and thus change the flow paths and, hence, substrate transport. This takes place when the detachment process is not strong enough to keep flow channels open. Depending on the application at hand, this can cause a serious drop in performance of the biofilm system.

Mathematical models of biofilms have been developed since the 1980s [11, 25, 37]. Despite newer two- and three-dimensional models that were proposed since the end of the 1990s, the one-dimensional biofilm model introduced in [37] is still the basis for many engineering applications. See also [5] for an early overview. It has been implemented in its original or extended form in numerous software packages that are more or less routinely used by wastewater engineers [2, 36]. The description of the complex physical detachment process in such one-dimensional models must be relatively simple and qualitatively phenomenological. In many cases, it is implemented as a sink term (*"volumetric detachment"* [17]). The hydrodynamic conditions that affect detachment are usually not explicitly considered, or at most implicitly by lumping reactor hydrodynamics into the constant detachment rate parameters. If the reactor and its operating conditions are such that biofilm growth does not significantly alter the shear forces acting on the biofilm, this is a good assumption. In other applications, however, this might not be sufficient. In these cases, the detachment rate functions used in the mathematical model should reflect the effect that a growing biofilm has on the local flow field. It can be argued that this is in particular important in porous medium applications, where flow channels can be clogged, or in applications, where biofouling is controlled mechanically, by increasing flow rates and thus detachment forces. Investigating the effect of the choice of detachment rate functions on the longterm behavior of the traditional biofim model is the primary goal of the present study. To this end we will analyse two flow rate dependent detachment rate functions that can be considered straightforward generalization of the current non shear dependent detachment models with constant coefficients.

The behavior of the traditional one-dimensional biofilm model with the commonly used non-shear dependent detachment rate functions is relatively well understood based on many numerical simulations that have been reported in the literature, but only very little is mathematically proven. The reason for this is likely that the general multi-species, multi-substrate biofilm model is a non-linear coupled hyperbolic-parabolic free boundary value problem, which is not easily accessible to a rigorous analysis. Early analytical studies focused on steady state solutions of a simple single-species model [24]. More recently an existence proof was given for a particular dynamic multi-species model application [31], and an exclusion principle was proved for a competition biofilm model [12]. Existence of a unique weak solution of a multi-dimensional generalization of the single-species biofilm model

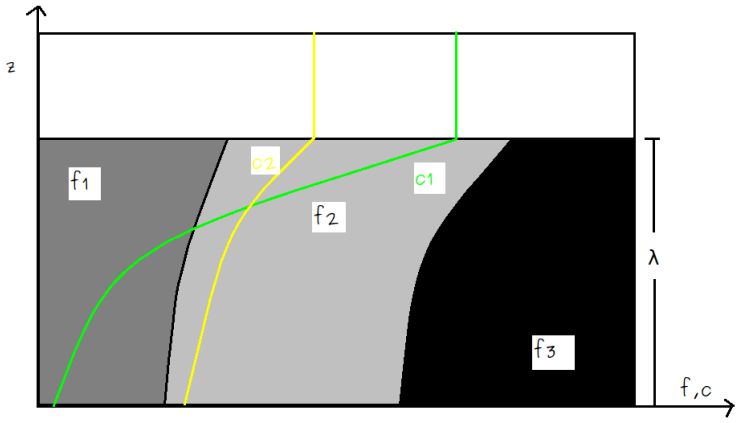


FIGURE 1. Schematic of a multi-species, multi-substrate biofilm as modeled by [37]. A biofilm of thickness $\lambda$ consists of particulate substances with volume fraction $f_i(z)$ (represented as gray/black shaded areas) with $\sum f_i = 1$. Growth is controlled by dissolved substrates with concentrations $c_i(z)$. In the aqueous bulk phase, the substrate concentrations are constant.

was analyzed in [21]. These previous studies used partial differential equations techniques to study the model. To study the effect of detachment and reactor hydrodynamics we take a different approach. We formally rewrite the single species biofilm model as a scalar ordinary differential equation, which we discuss with the usual techniques, in particular comparison theorems. We then use the results of the single-species model to infer the long term behavior of multi-species models by constructing upper and/or lower solutions.

2. **Governing equations.** Our study is based on the one-dimensional biofilm model of [37], assuming a homogeneous layer of biofilm covering the substratum. The biofilm *per se* is formed primarily by active bacteria and inert biomass. These are volume occupying particulate substances. The biofilm is assumed to be incompressible, i.e. the volume fraction occupied by the particulate substances add up to unity, see also the schematic in Figure 1. The EPS is usually subsumed in the active biomass, i.e. it is implicitly assumed that the biofilm-to-EPS ratio is constant (see [10] for an example where EPS is considered separately). The bacteria consume nutrients and other dissolved substrates, which diffuse from the aqueous phase into the biofilm. Consumption of nutrients leads to production of new biomass and thus to biofilm expansion.

We denote the volume fractions of the particulate substances by $f_i$, $i = 1, ..., n_f$ and the concentrations of the dissolved substrates by $c_i$, $i = 1, ..., n_c$. A straightforward mass balance for the biomass fractions gives

$$\frac{\partial f_i}{\partial t} + \frac{\partial}{\partial z}(u f_i) = R_i(f_1, ..., f_{n_f}; c_1, ..., c_{n_c}), \quad i = 1, ..., n_f, \quad 0 \le z \le \lambda(t) \qquad (1)$$

with the constraint

$$\sum_{i=1}^{n_f} f_i(t,z) \equiv 1, \quad 0 \le z \le \lambda(t)$$

which allows to eliminate one of the equations in (1). Here, the independent variable $t$ is time, and $z$ denotes the location in the one-dimensional biofilm, $0 \le z \le \lambda(t)$. The location $z = 0$ is at the substratum on which the biofilm grows, while $\lambda = \lambda(t)$ is the biofilm thickness, which changes in time due to biofilm growth and detachment. The terms $R_i$ on the right hand side are biomass growth and decay terms. The variable $u(t,z)$ is the velocity with which the biomass moves in the biofilm. Biomass movement is due to the expansion of the biofilm caused by local net growth, i.e. by the conversion of nutrients into new biomass,

$$u(t,z) = \int_0^z \sum_{i=1}^{n_f} R_i(f_1,...,f_{n_f};c_1,...,c_{n_c})dz. \tag{2}$$

In the biofilm, the dissolved substrates are subject to diffusion and reaction and described by

$$\frac{\partial c_i}{\partial t} = D_i \frac{\partial^2 c_i}{\partial z^2} + r_i(f_1,...f_{n_f},c_1,...,c_{n_c}), \quad \frac{\partial c_i}{\partial z}(t,0) = 0, \quad c_i(t,\lambda(t)) = S_i(t)$$

for $i = 1,...,n_c$. Assuming that external mass transfer resistance is negligible, $S_i$ is the bulk concentration. The diffusion coefficient for the $i$th substrate is denoted by $D_i$ and the reaction $r_i$ describes, e.g. depletion of substrate for growth of new biomass. They are usually coupled to the biomass production terms $R_i$. A standard time-scale argument that is frequently used in biofilm modeling [11, 36] allows us to consider the substrate equation in quasi-steady state, i.e. at time $t$ it simplifies to

$$0 = D_i \frac{\partial^2 c_i}{\partial z^2} + r_i(f_1,...,f_{n_f};c_1,...,c_{n_c}), \quad \frac{\partial c_i}{\partial z}(t,0) = 0, \quad c_i(t,\lambda(t)) = S_i(t) \tag{3}$$

The change of the biofilm thickness is determined by net growth, i.e. the net production/decay of new biomass and by detachment. Assuming volumetric detachment as described in [17], we obtain

$$\frac{d\lambda}{dt} = u(t,\lambda(t)) - d(\lambda)\lambda, \tag{4}$$

where the function $d(\lambda)$ is the volumetric detachment rate at which biomass is eroded or sloughed off from the biofilm.

In the case of a single-species biofilm that is controlled only by one dissolved substrate, i.e. $n_f = n_c = 1$, this model simplifies greatly. Since $f_1 \equiv 1$, the equations (1) and (2) are equivalent, and the biofilm model reduces to

$$\frac{d}{dt}\lambda = \int_0^\lambda R(c)dz - d(\lambda)\lambda \tag{5}$$

The standard reaction kinetics used in biofilm modeling is Monod kinetics, according to which the consumption rate is given by

$$r_i(c) = -\frac{\mu X_\infty}{Y}\frac{c}{\kappa + c}. \tag{6}$$

The net growth rate is the sum of biomass production and cell death or lysis,

$$R_i(c) = \mu\frac{c}{\kappa + c} - k_d. \tag{7}$$

Here, constant $\mu$ is the maximum specific growth rate, $X_\infty$ is the maximum biomass density, $Y$ a yield coefficient, $\kappa$ the Monod half saturation concentration, and $k_d$ the decay rate. Thus, the substrate concentration $c$ is described by the two-point boundary value problem

$$D\frac{d^2c}{dz^2} = \frac{k_1 c}{\kappa + c}, \quad \frac{dc}{dz}(0) = 0, \quad c(\lambda) = S, \tag{8}$$

with $k_1 = \mu X_\infty / Y$. Hence, the single species biofilm model (5) reads

$$\frac{d}{dt}\lambda = \int_0^\lambda \left(\frac{\mu c}{\kappa + c} - k_d\right) dz - d(\lambda)\lambda; \quad \lambda(0) = \lambda_0. \tag{9}$$

We observe that integrating (8) over the biofilm thickness and using the boundary conditions, we obtain

$$\int_0^\lambda \frac{\mu c}{\kappa + c} = \frac{DY}{X_\infty}\frac{dc}{dz}(\lambda) =: j(\lambda, S). \tag{10}$$

In order to evaluate $j(\lambda, S)$, the two-point boundary value problem for $c$ must be solved. Thus (9) becomes formally

$$\frac{d\lambda}{dt} = j(\lambda, S) - k_d\lambda - d(\lambda)\lambda. \tag{11}$$

A number of possible candidates for the detachment rate function $d(\lambda)$ have been proposed in the literature, which we will consider here:

$$\begin{cases} d_1(\lambda) &= \delta, \\ d_2(\lambda) &= \delta\lambda, \\ d_3(\lambda) &= \delta\tau^\gamma, \quad 0 < \gamma < 1, \\ d_4(\lambda) &= \delta\tau\lambda. \end{cases} \tag{12}$$

By $\delta$ we denote a constant detachment rate coefficient. We use the same symbol for each detachment rate model although we point out that both its dimensional unit and its numerical value is different for different $d_i$, $i = 1, ..., 4$. It can be assumed to be positive in all cases.

In $d_1$ the detachment rate is constant. This has been used previously in several studies, including [23, 28, 33]. In $d_2$ the detachment rate grows proportionally with the biofilm thickness. This criterion has become the *de facto* standard detachment criterion. It has been proposed in [34] and used since in numerous studies, such as [3, 36, 37] and many investigations that use existing biofilm modeling software packages

The detachment rate $d_3$ accounts for the experimental observation that the detachment rate depends on the bulk flow hydrodynamics. In this expression $\tau$ is the hydrodynamic shear rate acting on the biofilm. It changes as the biofilm grows, i.e. $\tau = \tau(\lambda)$. It also depends on the reactor type and operating conditions. The exponent $\gamma$ has been derived from experimental data, a default value is $\gamma = 0.58$ [26].

Finally, the detachment rate function $d = d_4(\lambda) = \delta\tau\lambda$ is proposed here. In this formulation, the detachment rate is assumed to depend on both, the biofilm itself and the hydrodynamic shear rate. This reflects recent experimental observations that biofilms are stronger in the inner layers than in the outer layers and that well developed thicker biofilms slough off easier than thin biofilms [8, 29].

If the shear rate $\tau$ is approximated by the (constant, i.e. independent of $\lambda$) reactor shear rate, then $\delta_3$ becomes equivalent with $\delta_1$ and $\delta_4$ becomes $\delta_2$.

The flux function $j(\lambda, S)$ is continuous, differentiable, strictly monotonic increasing in both it arguments and satisfies $j(0,\cdot) = 0$, $j(\cdot, 0) = 0$ [16]. Using comparison theorems for Sturm-Liouville type problems, e.g. [4, 35], it is found in [16] that

$$S\sqrt{\frac{\mu}{K+S}}\tanh\sqrt{\frac{\lambda^2\mu}{K+S}} \le j(\lambda, S) \le S\sqrt{\frac{\mu}{K}}\tanh\sqrt{\frac{\lambda^2\mu}{K}}. \tag{13}$$

Moreover, [16] derives the estimates

$$\mu\frac{S}{K} \ge j_\lambda(0, S) \ge \mu\frac{S}{K+S}. \tag{14}$$

In particular, (13) indicates that the function $j(\lambda,\cdot)$ is bounded by a positive constant that depends only on model parameters.

It is easy to verify the following result with standard arguments.

**Proposition 1.** *If $d(\lambda)$ is continuously differentiable with respect to $\lambda$, then the initial value problem of (11) with $\lambda(0) = \lambda_0 > 0$ possesses a unique positive solution, and $\lambda = 0$ is an equilibrium.*

The hypothesis of the preceding Proposition 1 is trivially satisfied for the detachment rate function $d_1$ and $d_2$, which do not depend on the bulk flow hydrodynamics. For the detachment rate functions $d_3$ and $d_4$, Proposition 1 poses conditions on the shear stress function $\tau(\lambda)$, which depends on the reactor and its operating conditions.

For the two cases in which the detachment rate function does not depend on the hydrodynamics the long term behavior is easily characterized:

**Proposition 2.** *For model (11) with detachment rate function $d(\lambda) = d_1(\lambda) = \delta$, the trivial equilibrium $\lambda = 0$ is asymptotically stable if $k_d+\delta > j_\lambda(0, S)$, and unstable if the $k_d + \delta < j_\lambda(0, S)$. In the latter case, there exists a positive, asymptotically stable equilibrium $\lambda^* > 0$.*

*If instead we consider detachment rate functions $d(\lambda) = d_2(\lambda) = \delta\lambda$, then the trivial equilibrium $\lambda = 0$ is asymptotically stable if $k_d > j_\lambda(0, S)$ and unstable if $k_d < j_\lambda(0, S)$. In the latter case, there exists a positive, asymptotically stable equilibrium $\lambda^* > 0$.*

*Proof.* We consider first the case $d(\lambda) = d_1(\lambda) = \delta$. The right-hand-side of (11) is

$$F(\lambda) = j(\lambda, s) - (k_d + \delta)\lambda.$$

thus for the trivial equilibrium we have

$$F'(0) = j_\lambda(0, s) - (k_d + \delta),$$

from which follows that the trivial equilibrium is asymptotically stable for $k_d + \delta > j_\lambda(0, S)$ and unstable if $k_d + \delta < j_\lambda(0, S)$. The function $j(\lambda, S)$ is monotonic increasing and bounded by a positive constant. Thus, if $k_d + \delta < j_\lambda(0, S)$, then the function $(k_d + \delta)\lambda$ will intersect with $j(\lambda, S)$ from below at least once, say in a point $\lambda^*$. Then $j_\lambda(\lambda^*, S) < (k_d + \delta)\lambda^*$. Thus, this intersection is an asymptotically stable equilibrium.

The case $d(\lambda) = d_2(\lambda) = \delta\lambda$ follows with the same monotonicity arguments. The only difference is that the function $j(\lambda, S)$ is compared against the quadratic function $k_d\lambda + \delta\lambda^2$ instead of the linear function $(k_d + \delta)\lambda$. □

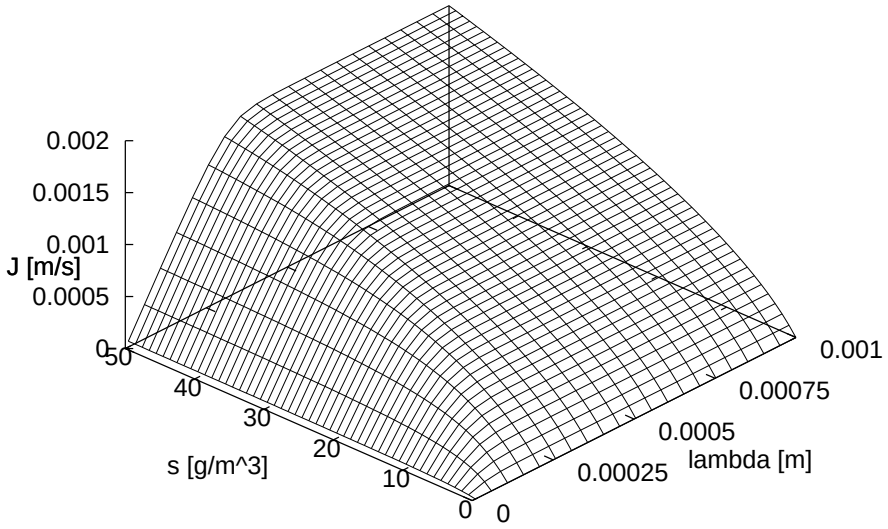


FIGURE 2. Numerical calculation of the specific flux $j(\lambda, S)$ for the parameters in Table 1.

**Remark 1.** It follows with the same geometrical arguments that for $d(\lambda) = d_1(\lambda)$ there is no positive equilibrium if $k_d + \delta > j_\lambda(0, S)$.

Since we only established monotonicity and boundedness of the flux function $j(\lambda, S)$, we cannot exclude the possibility that there might be several non-trivial equilibria. However, if, like its upper and lower bounds given above, the second derivative $j_{\lambda\lambda}(\lambda, S)$ is also non-positive, then equilibrium $\lambda^*$ is unique. That this is the case is suggested by numerical simulations of (8) that we carried out for the parameters in Table 1 with $0 \leq \lambda \leq 10^{-3}m$ and $0 \leq s \leq 50g/m^3$. The results, shown in Figure 2, indicate that $j_{\lambda\lambda}(\lambda, S) \leq 0$.

Our results indicate that for $d = d_1$ or $d = d_2$ the trivial equilibrium, i.e. washout of the biofilm, is stable if the biomass growth terms are dominated by the biomass loss terms. This is for example the case if the bulk substrate concentration is sufficiently small. In the case of the linear detachment model with $d(\lambda) = d_1(\lambda) = \delta$ washout occurs if the biomass production rate is smaller than the sum of both biomass loss terms, lysis and detachment. On the other hand, if the standard quadratic detachment model $d(\lambda) = d_2(\lambda) = \delta\lambda$ is used, only the balance between growth and lysis determines whether the biofilm washes out, independent of the detachment coefficient $\delta$.

The situation is more involved for the detachment rate functions $d(\lambda) = d_i(\lambda)$ with $i = 3, 4$, which also depend on the hydrodynamic conditions. These are affected by the reactor used. In all cases the shear stress $\tau$ must be computed. We will do this for three reactor types in the next section.

## 3. Shear rate functions for idealized hydrodynamic scenarios.

We consider three formulations for the shear rate $\tau(\lambda)$ at the biofilm/liquid interface that enters

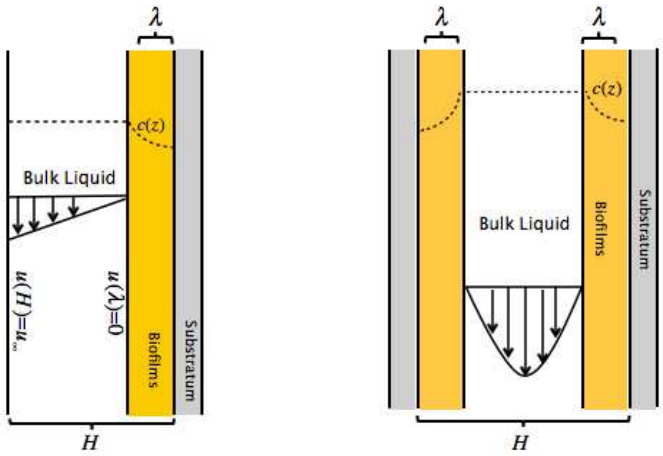


FIGURE 3. Schematic of flow reactors: Couette flow (left): A biofilm of thickness $\lambda$ grows on the stationary plate; the opposite plate moves with constant velocity inducing a linear flow profile; also indicated is the substrate concentration as dotted line. Poiseuille flow (right): Biofilm of thickness $\lambda$ forms on both walls; the flow profile in the channel is quadratic; also indicated is the substrate concentration as dotted line.

the detachment rate functions $d_3(\lambda)$ and $d_4(\lambda)$. One models Couette flow between two parallel plates, one of which moves with a constant velocity. This mimics the hydrodynamic scenario in a rotating drum or roto torque biofilm reactor with narrow gap or in a gap between moving parts of industrial or food processing equipment. The other two formulations are concerned with Poiseuille flow between two stationary parallel plates. In one case the flow is controlled by prescribing the flow rate through the channel, in the other one the flow is driven by prescribing the (constant) pressure gradient. The former can be understood as an idealization of a microfluidics biofilm reactor, the latter of a trickling filter or a porous medium biofilm reactor. See Figure 3 for a schematic representation of these setups.

We work with the elementary, well-known analytical solutions of the two dimensional Navier-Stokes equations for these two hydrodynamic setups, which can be found e.g. in [20]. These are valid for laminar flows, i.e. for Reynolds numbers below the transition to turbulent flow and the onset of Taylor instabilities for Couette flow. For many biofilm applications, both in the real world or in a laboratory setting, these are not severe limitations.

3.1. **Couette flow.** We consider laminar flow between two parallel plates, the top of which moves with prescribed velocity $u_\infty$, see Figure 3 (left panel). On the bottom plate we assume a biofilm of thickness $\lambda$. The flow profile is given then by the linear function

$$u(z) = \frac{z-\lambda}{H-\lambda} u_\infty,$$

from which we compute the shear stress at the biofilm/liquid interface as

$$\tau_0(\lambda) = \eta \left.\frac{du}{dz}\right|_\lambda = \eta \frac{u_\infty}{H-\lambda}, \tag{15}$$

where $\eta$ is the dynamic viscosity of the fluid. Thus, the shear force acting on the biofilm increases as the biofilm grows. If $\lambda = H$ the channel clogs and the model breaks down.

3.2. **Poiseuille flow.** We consider flow between two parallel, stationary plates, a distance $H$ apart. On each plate a biofilm with thickness $\lambda$ is assumed, see Figure 3 (right panel). The flow velocity is given by the parabolic profile

$$u(z) = \frac{1}{2\eta}\nabla P\left(z^2 - Hz + \lambda(H-\lambda)\right)$$

where $\nabla P$ is the constant (negative) pressure gradient along the channel and $\eta$ again the viscosity of the liquid. We replace $\nabla P$ by the new positive parameter

$$\psi := -\nabla P.$$

For reasons of symmetry we can restrict ourselves to studying only one of the biofilm interfaces, namely the one at $z = \lambda$. The results hold analogously for the one at $z = H - \lambda$. The shear stress at the biofilm/liquid interface is then

$$\tau_1 = \eta \left.\frac{du}{dz}\right|_\lambda = \psi\left(\frac{H}{2} - \lambda\right) \tag{16}$$

Poiseuille flow can be driven by two mechanisms, which are equivalent in an empty channel without biofilm. One is to prescribe the specific flow rate $q = \int_\lambda^{H-\lambda} u dy$ per unit width of the flow channel, the other one is to apply a pressure drop, i.e. to prescribe the parameter $\psi$. Both quantities are related by

$$q = \frac{\psi}{12\eta}\left(\frac{H}{2} - \lambda\right)^3. \tag{17}$$

If the flow is driven by prescribing the flow rate, (16) becomes

$$\tau_2(\lambda) = \frac{12\eta q}{\left(\frac{H}{2} - \lambda\right)^2}. \tag{18}$$

In the case of a pressure drop driven flow, the shear rate $\tau_1(\lambda)$ decreases as the biofilm grows, reflecting that the growing biofilm obstructs the flow and the flow velocity and flow rate decrease. In a flow rate driven regime, the shear force $\tau_2(\lambda)$ acting on the biofilm increases, reflecting that a narrower flow path leads to increased flow velocities if the flow rate remains constant. In both cases the biofilm reaching $\lambda = H/2$ marks a complete clogging of the pore space and a breakdown of the model.

4. **Analysis of biofilm models with shear-dependent detachment rates.** In this section we investigate how the choice of a detachment rate function and the hydrodynamic conditions affect the longterm prediction of the single-species biofilm model. We first study under which conditions the solutions of the model exist globally, are non-negative and bounded from above by a maximum biofilm height that would mark complete clogging of the flow channel.

**Proposition 3.** *The solutions of the biofilm model (11) with detachment rate function $d(\lambda) = d_i(\lambda)$, $i = 3, 4$, shear rate $\tau_0(\lambda)$, and initial data $\lambda(0) = \lambda_0 \in (0, H)$ remain in $[0, H)$. They exist for all $t > 0$, are unique, monotonic, and converge to a stable equilibrium $\lambda^* \in [0, H)$*

*Proof.* Let $\lambda(t)$ be a solution of (11) with $0 < \lambda(0) < H$ and let $\hat{\lambda}$ be the solution of the initial value problem

$$\frac{d\hat{\lambda}}{dt} = \kappa - d(\hat{\lambda})\hat{\lambda}, \quad \hat{\lambda}(0) = \lambda_0,$$

with $\kappa := j(H, S)$. Note that $\hat{\lambda}$ exists and is unique, because $d(\lambda)$ is continuously differentiable for all $0 < \lambda < H$. Then by comparison $\hat{\lambda}(t) \geq \lambda(t)$ for all $t > 0$. We note that the function $d(\lambda)$ is monotonically increasing and $d(\lambda)\lambda \to \infty$ as $\lambda \to H$. Thus, there exists a constant $\bar{\lambda}$, $0 < \bar{\lambda} < H$, such that

$$\frac{d\hat{\lambda}}{dt} = \kappa - d(\hat{\lambda})\hat{\lambda} < 0$$

for all $\hat{\lambda} > \bar{\lambda}$.

Similarly, it is easy to verify with standard comparison arguments that the trivial steady state solution $\tilde{\lambda} \equiv 0$ is a lower bound on $\lambda(t)$. Thus,

$$0 \leq \lambda(t) \leq \hat{\lambda}(t) \leq \max\{\bar{\lambda}, \lambda_0\}.$$

Since the detachment rate is differentiable in $(0, H)$ model (11) satisfies a Lipschitz condition which implies the existence of a unique solution to the initial value problem. This solution is bounded from above and below by constants and exists globally. It is monotonic and converges to an equilibrium. □

**Proposition 4.** *The solutions of the biofilm model (11) with detachment rate function $d(\lambda) = d_i(\lambda)$, $i = 3, 4$, shear rate $\tau_2(\lambda)$, and initial data $\lambda(0) = \lambda_0 \in (0, H/2)$ remain in $[0, H/2)$. They exist for all $t > 0$, are unique, monotonic, and converge to a stable equilibrium $\lambda^* \in [0, H/2)$.*

The argumentation is the same as in the previous Proposition 3. The only difference is that the shear rate function $\tau_2$ has a singularity at $\lambda = H/2$, not at $\lambda = H$.

The preceding propositions show that for Couette flow or for flow rate driven Poiseuille flow the channel never clogs. This does not necessarily carry over to pressure drop driven Poiseuille flow, i.e. the shear rate $\tau_1(\lambda)$, for which the interval $(0, H/2)$ is not necessarily positively invariant. Thus, for some parameters some solutions starting in $(0, H/2)$ may reach $\lambda = H/2$. This indicates complete clogging of the channel and marks a break down of the model.

**Remark 2.** Model (11) with detachment rate function $d(\lambda) = d_3(\lambda)$ or $d(\lambda) = d_4(\lambda)$ and shear rate $\tau_1(\lambda)$ has a positively invariant interval $[0, \lambda^*]$ with an asymptotically stable equilibrium $\lambda^* < H/2$, if the constant $\alpha := \frac{1}{2}\delta\rho\psi$ is large enough, where large values for $\alpha$ indicate high detachment forces. Inequalities (13) can be used to compute a necessary lower and a sufficient upper estimate for the critical value of $\alpha$.

An important question is the question whether a biofilm can establish itself, i.e. the stability of the trivial equilibrium $\lambda = 0$.

**Proposition 5.** *For model (11) with detachment rate function $d(\lambda) = d_3(\lambda) = \delta\tau^\nu$, the trivial equilibrium $\lambda = 0$ is asymptotically stable if $k_d + \delta\tau(0)^\nu > j_\lambda(0, S)$ and unstable if $k_d + \delta\tau(0)^\nu < j_\lambda(0, S)$. In the latter case, there exists a positive, asymptotically stable equilibrium $\lambda^* > 0$.*

*If instead we consider detachment rate functions $d(\lambda) = d_4(\lambda) = \delta\lambda\tau$, then the trivial equilibrium $\lambda = 0$ is asymptotically stable if $k_d > j_\lambda(0, S)$ and unstable*

*if $k_d < j_\lambda(0,S)$. In the latter case, there exists a positive, asymptotically stable equilibrium $\lambda^* > 0$.*

*Proof.* The right-hand-side of (11) is

$$F(\lambda) = j(\lambda, s) - (k_d + d(\lambda))\lambda.$$

thus

$$F'(\lambda) = j_\lambda(\lambda, s) - k_d - d'(\lambda)\lambda - d(\lambda)$$

and for the trivial equilibrium

$$F'(0) = j_\lambda(0, s) - k_d - d(0)$$

The assertion follows with $d_3(0) = \delta\tau(0)^\nu$, $d_4(0) = 0$. □

Note that the preceding result is independent of the particular shear-rate function chosen and holds for all $\tau(\lambda) = \tau_i(\lambda)$ with $i = 0, 1, 2$.

Proposition 5 is easily generalized: If the detachment function is $d(\lambda) = \mathcal{O}(\lambda)$, then the stability of the trivial equilibrium depends only on growth and lysis parameters, but not on the coefficients of the detachment function or on the hydrodynamic conditions. On the other hand, if $d(\lambda) = \mathcal{O}(1)$ then these factors can be a deciding factor whether or not a biofilm can develop. Thus, prediction of persistence or washout of a biofilm can be sensitive to the choice of detachment rate used in a modeling study. Under this light, $d_3$ can be viewed as a shear-stress dependent generalization of the more frequently used expression $d_1$, and $d_4$ as generalization of detachment rate function $d_2$, which is used as the *de facto* standard detachment model in 1D biofilm simulation studies.

Propositions 3 and 4 showed that under Couette flow or under flow rate driven Poiseuille flow the biofilm thickness $\lambda$ attains eventually an equilibrium $\lambda^*$. Proposition 5, together with estimate (14) allows to decide whether this equilibrium will be the trivial one, $\lambda^* = 0$, or a non-trivial one, $\lambda^* > 0$. In the latter case it remains open whether this equilibrium is unique or whether the longterm behavior depends on the initial data. Computer simulations indicate that $j(\lambda, S)$, as a function of $\lambda$, like its upper and lower estimates according to (13) is concave, see Figure 2. If this is the case, it suffices for $d(\lambda)$ to be convex that the equilibrium $\lambda^*$ is unique. The detachment rate functions $d(\lambda) = d_3(\lambda) = \delta\tau(\lambda)^\gamma$ and $d(\lambda) = d_4(\lambda) = \delta\lambda\tau(\lambda)$ satisfy this condition for both shear rate expressions $\tau = \tau_0(\lambda)$ and $\tau = \tau_2(\lambda)$. On the other, hand with the shear rate expression $\tau = \tau_1(\lambda)$ this condition is not satisfied. In this case it depends on the circumstances, i.e. parameters, whether a stable equilibrium exists in the interval $(0, H/2)$. If $\alpha$ is large enough in the sense of Remark 2, then this is the case, but there could be also another, unstable equilibrium $\lambda^* < \lambda^{**} < H/2$.

## 5. **Extensions of the biofilm model.**

### 5.1. **Application to multi-species models.**

In many relevant applications, the biofilm communities are formed by several bacterial species and controlled by several dissolved substrates, while the results of sections 2 and 4 have been derived explicitly for the simpler single-species, single-substrate case. Some of the results, however, can be carried over qualitatively to more complex scenarios. For instance, often we can find a single-species biofilm model which provides an upper estimate for the thickness of a multi-species biofilm model. This is usually possible if the biomass

reaction rates are bounded, which for most practical applications is not a severe restriction. We demonstrate this for two examples.

5.1.1. *A heterotrophic-autotrophic biofilm for wastewater treatment.* First, we consider a multi-species biofilm system consisting of aerobic heterotrophic bacteria, aerobic autotrophic nitrifiers and inert biomass. Such systems arise in the modeling of wastewater treatment processes. The growth of the active biomass fractions is controlled by the dissolved substrates oxygen, carbon, and ammonium. Both active species compete for oxygen. The growth of the nitrifiers is also controlled by ammonium availability, the growth of the heterotrophs by carbon availability. Respiration of both active biomass fractions is controlled by oxygen availability. Lysed active biomass is converted into inactive biomass. This model has been introduced in [37] and was also the basis of the multi-species Benchmark Problem 3 of the IWA Water Association's Taskgroup on Biofilm Modeling [27, 36].

We denote by $f_{1,2,3}$ the densities of heterotrophs, autotrophs and inerts, by $c_{1,2,3}$ the concentrations of oxygen, carbon, and ammonium. The bulk concentrations we denote accordingly by $S_{1,2,3}$. Starting point for the analysis of the multi-species case are the equations (2) and (4).

Following [36, 37], the growth functions $R_{1,2,3}$ are

$$\begin{aligned} R_1 &= \mu_1 f_1 \frac{c_1}{K_{11}+c_1}\frac{c_2}{K_2+c_2} - k_1 f_1 - l_1 f_1 \frac{c_1}{K_{11}+c_1}, \\ R_2 &= \mu_2 f_2 \frac{c_1}{K_{21}+c_1}\frac{c_3}{K_3+c_3} - k_2 f_2 - l_2 f_2 \frac{c_1}{K_{21}+c_1}, \\ R_3 &= k_1 f_1 + k_2 f_2, \end{aligned}$$

where $\mu_{1,2}$ are the maximum specific growth rates of the active species, $k_{1,2}$ the lysis rates, $l_{1,2}$ the respiration rates, and $K_{ij}$ and $K_i$ are half saturation concentrations. These parameters are non-negative.

From the non-negativity of biomass densities $f_{1,2,3}$ and substrate concentrations $c_{1,2,3}$ we obtain

$$R_1 + R_2 + R_3 \le \mu(f_1+f_2)\frac{c_1}{K+c_1}$$

where $\mu := \max\{\mu_1 - l_1, \mu_2 - l_2\}$ and $K := \min\{K_{11}, K_{21}\}$. Hence, with (4) and $f_1 + f_2 + f_3 = 1$ we have for the biofilm thickness

$$\frac{d\lambda}{dt} \le \int_0^\lambda \frac{\mu c_1}{K+c_1} dz - d(\lambda)\lambda. \tag{19}$$

The oxygen concentration $c_1$ satisfies the two-point boundary value problem

$$\frac{d^2 c_1}{dz^2} = \alpha f_1 \frac{c_1}{K_{11}+c_1}\frac{c_2}{K_2+c_2}$$

with

$$\frac{dc_1}{dz}(0) = 0, \quad c_1(\lambda) = S_1,$$

where the parameters growth rate, yield coefficient, diffusion coefficient are subsumed in the new constant parameter $\alpha$. Using again that $0 \le \frac{c_2}{K_2+c_2} \le 1$, we find with the standard comparison theorems for two-point boundary value problems [4, 35], that the solution $\tilde{c}$ of the two-point boundary value problem

$$\frac{d^2\tilde{c}}{dz^2} = \alpha f_1 \frac{\tilde{c}}{K_{11}+\tilde{c}}, \quad \frac{d\tilde{c}}{dz}(0) = 0, \quad \tilde{c}(\lambda) = S_1,$$

is a lower estimate for $c_1$, i.e.

$$\tilde{c}(z) \le c_1(z) \quad \text{for} \quad 0 \le z \le \lambda.$$

Therefore, with $\tilde{c}(\lambda) = c_1(\lambda) = S_1$ we obtain for the substrate flux at the interface between biofilm and water

$$\frac{d\tilde{c}}{dz}(\lambda) \ge \frac{dc_1}{dz}(\lambda).$$

Thus we obtain from (19) the differential inequality

$$\frac{d\lambda}{dt} \le \tilde{j}(\lambda, S) - d(\lambda)\lambda \tag{20}$$

where we used the short hand notation

$$\tilde{j}(\lambda, S) := \frac{1}{\alpha}\frac{d\tilde{c}}{dz}(\lambda).$$

We denote by $\tilde{\lambda}$ the solution of the associated initial value problem

$$\frac{d\tilde{\lambda}}{dt} = \tilde{j}(\tilde{\lambda}, S) - d(\tilde{\lambda})\tilde{\lambda}, \quad \tilde{\lambda}(0) = \lambda_0.$$

By comparison we have $\tilde{\lambda}(t) > \lambda(t)$. For the flow rate driven Poiseuille flow mechanism Proposition 4 showed that the biofilm will eventually attain a thickness $\tilde{\lambda}^* < H/2$, i.e. that the channel will not clog. Since the single species biofilm thickness $\tilde{\lambda}$ is an upper estimate for the multi-species biofilm thickness $\lambda$, the same holds true for the multi-species case. A similar result follows with Proposition 3 for the Couette mechanism.

Moreover, if on the other hand in the case $d(\lambda) = d_4(\lambda)$ and the flow rate and detachment parameters are such that the upper estimate $\tilde{\lambda}$ converges to the trivial equilibrium, then also the multi-species biofilm cannot establish itself.

5.1.2. *A biobarrier biofilm for groundwater protection.* The same result can be obtained with analogous arguments for many other biofilm systems. The question of bioclogging of flow channels is of great importance in bioremediation technologies or for biobarriers for groundwater protection. One such system is the dual-species biobarrier biofilm formed by *Klebsiella oxytoca* and *Burkholderia cepacia* [6, 7, 18, 19]. The latter removes the pollutant TCE but is a weak biofilm producer. The former is a prolific biofilm producer that does not degrade the pollutant but stabilizes the biofilm. Both species compete for a common resource. The growth functions for this dual species biobarrier biofilm according to [6, 7] are

$$\begin{aligned} R_1 &= \mu_1 f_1 \frac{c_1}{K_{11} + c_1} - k_1 f_1, \\ R_2 &= \mu_2 f_2 \frac{c_1}{K_{21} + c_1}\frac{c_2}{K_2 + c_2} - k_2 f_2, \end{aligned}$$

where $f_1$ and $f_2$ are the densities of *K.oxytoca* and *B.cepacia*, and $c_1$ and $c_2$ are the concentrations of nutrient and pollutant. The flow between soil particles can be approximated by Poiseuille flow. We obtain the estimate

$$R_1 + R_2 \le \mu \frac{c_1}{K + c_1} - k$$

with $\mu := \max\{\mu_1, \mu_2\}$, $K := \min\{K_{11}, K_{21}\}$ and $k := \min\{k_1, k_2\}$. The same arguments as above lead to the conclusion that soil pores remain open if the flow is driven by a fixed rate, but might clog if the flow is driven by a too low pressure difference.

5.2. **Application to a simple reactor model.** In the previous sections we assumed that the bulk substrate concentration does not noticeably change in response to biofilm accumulation. In many other applications it is more realistic to account for the bulk substrate to be depleted due to biofilm growth. We formulate a simple model for such a flow chamber reactor. Assuming the bulk to be completely mixed, the equation governing the concentration $S$ in the aqueous phase is derived from the basic reactor mass balance, stating that the amount of substrate equals inflow minus outflow and consumption by the biofilm. The latter can be expressed in terms of the substrate flux into the biofilm, i.e. in terms of $j(\lambda, S)$. This substrate equation is coupled with the equation for the biofilm thickness. We obtain

$$\frac{d}{dt}\begin{pmatrix} VS \\ \lambda \end{pmatrix} = \begin{pmatrix} Q(\lambda)\,(S_\infty - S) - \frac{X_\infty L}{Y} j(\lambda, S) \\ j(\lambda, S) - k\lambda - d(\lambda)\lambda \end{pmatrix}, \tag{21}$$

where $Q = Q(\lambda)$ is the specific flow rate (per unit width) in the reactor and $V = (H-2\lambda)L$ is the specific volume (per unit width) of the aqueous phase; $L$ denotes the length of the flow chamber. By $S_\infty$ we denote the substrate inflow concentration. Note that by writing $Q = Q(\lambda)$ we emphasize that in the case of a Couette reactor or of pressure drop driven Poiseuille flow the flow rate depends on the biofilm thickness. In the case of flow rate driven Poiseuille flow, this simplifies with $Q = const.$

After rearranging terms, equation (21) can be rewritten as

$$\frac{d}{dt}\begin{pmatrix} S \\ \lambda \end{pmatrix} = \begin{pmatrix} \frac{1}{H-2\lambda}\left(\frac{Q(\lambda)}{L}\,(S_\infty - S) - \frac{X_\infty}{Y} j(\lambda, S) + 2S\,[j(\lambda, S) - k\lambda - d(\lambda)\lambda]\right) \\ j(\lambda, S) - k\lambda - d(\lambda)\lambda \end{pmatrix}. \tag{22}$$

Since $j(\lambda, S) \geq 0$, it follows with the usual comparison arguments that $0 \leq S(t) \leq S_{\max} := \max\{S_\infty, S_0\}$ for all $t > 0$, if the initial data satisfy $S(0) := S_0 \leq \frac{X_\infty}{2Y}$ and if $S_\infty < \frac{X_\infty}{2Y}$. The last two condition are not a severe restriction for realistic biofilm systems, see also Table 1. Thus with $S \leq S_{max}$ an upper estimate on the biofilm thickness can be derived as the solution $\tilde{\lambda}$ of

$$\frac{d\tilde{\lambda}}{dt} = j(\tilde{\lambda}, S_{max}) - k\tilde{\lambda} - d(\tilde{\lambda})\tilde{\lambda}, \quad \tilde{\lambda}(0) = \lambda_0. \tag{23}$$

Hence, similar as in the case of the multi-species model, if the above single species model for $\tilde{\lambda}$ predicts that the flow channel does not clog, then neither does the channel clog for the system (21). This is the case, e.g. for $d(\lambda) = d_3(\lambda)$ or $d(\lambda) = d_4(\lambda)$ with shear rate $\tau_0(\lambda)$ or $\tau_2(\lambda)$. Similarly, if $\tilde{\lambda}$ converges to 0, then $\lambda$ will as well.

The reactor model (21) always has the trivial equilibrium $(S^*, \lambda^*) = (S_\infty, 0)$, independent of the detachment rate and shear stress model. While the Jacobian of (22) yields a lengthy expression (see (30) in the Appendix), it simplifies for the trivial equilibrium and is obtained as

$$F'(S_\infty, 0) = \begin{pmatrix} -\frac{Q(\lambda)}{V} & * \\ 0 & j_\lambda(0, S_\infty) - k - d(0) \end{pmatrix} \tag{24}$$

where we used that $j_S(0, S) = 0$ [16]. Thus, we always have the negative eigenvalue $z_1 = -Q/V$. The sign of the second eigenvalue depends on the parameters. Note that the results of Proposition 5 carry over. Hence, if the trivial equilibrium is stable for (23), then it is also stable for (21) and *vice versa*.

The existence and stability of non-trivial equilibria of (21) can formally be studied using phase plane analysis. However, due to the number of parameters involved and

due to the algebraic complexity of some expressions, depending on the choice of detachment and shear rate functions, a complete analysis that lends itself to useful general existence and stability results is not feasible. We focus on the case that is not covered by the remark above, namely pressure gradient driven Poiseuille flow with shear rate model $\tau = \tau_1(\lambda)$. We investigate this for detachment rate function $d = d_3(\lambda)$. Recall that in the case of a constant bulk concentration we could not derive a general result about the possibility of the channel to be clogged, but found that it depends on the specific parameter choices.

We normalize the biofilm thickness with respect to $H/2$, and the bulk concentration with respect to $S_\infty$, i.e. we introduce the new dependent variables

$$s := \frac{S}{S_\infty}, \quad l := \frac{\lambda}{H/2}.$$

Furthermore, for algebraic simplicity we approximate the flux of substrate into the biofilm as

$$j(\lambda, S) \approx \mu \frac{\lambda S}{K + S}. \tag{25}$$

This value is exact if one uses $0th$ order kinetics instead of Monod kinetics, but it overestimates substrate consumption where $0th$ order kinetics does not approximate the Monod kinetics well. However, in [1] it was shown that (25) can be an acceptable flux approximation for realistically relevant parameters. Moreover, again for algebraic simplicity, we choose for the shear exponent $\nu = 1/2$, in good agreement with the value $\nu = 0.58$ suggested in [26]. Then, (22) becomes

$$\frac{d}{dt}\begin{pmatrix} s \\ l \end{pmatrix} = \begin{pmatrix} \alpha\psi(1-l)^2(1-s) - \beta\frac{l}{1-l}\frac{s}{\kappa+s} + \frac{2s}{1-l}\frac{dl}{dt} \\ \mu\frac{ls}{\kappa+s} - kl - \phi\sqrt{\psi}\sqrt{1-l}l \end{pmatrix}, \tag{26}$$

where the new compounded model parameters are

$$\alpha := \frac{H^2}{96\eta L}, \quad \beta := \frac{X_\infty \mu}{2Y S_\infty}, \quad \phi := \delta\sqrt{\frac{H}{2}}, \quad \kappa := \frac{K}{S_\infty}.$$

In the sequel we will treat the reaction parameters as given and investigate how the longterm behavior depends on the parameters that directly affect detachment, namely $\phi$ and $\psi$. We may assume without loss of generality that

$$\frac{\mu}{\kappa + 1} > k,$$

because otherwise cell death would dominate growth even under ideal food conditions and no biofilm would be able to establish, regardless of detachment effects.

The trivial equilibrium $(s^*, l^*) = (1, 0)$ is asymptotically stable if

$$\frac{\mu}{\kappa + 1} - k < \phi\sqrt{\psi}, \tag{27}$$

i.e if the detachment rate and the pressure gradient that drives the flow are sufficiently large. The trivial equilibrium is unstable if the reverse inequality holds.

We are interested in equilibria $(s^*, l^*) \in (0, 1) \times (0, 1) =: I$. These are the intersections of $l$-nullclines and $s$-nullclines, i.e of the curves in $I$ along which $dl/dt \equiv 0$ and $ds/dt \equiv 0$, respectively.

In $I$, the $l$-nullcline, parameterized as $l_2(s)$, can be found as

$$l_2(s) = 1 - \frac{1}{\phi^2\psi}\left(\frac{\mu s}{\kappa + s} - k\right)^2. \tag{28}$$

Let $\hat{s}$ be defined as the unique value with

$$\frac{\mu\hat{s}}{\kappa+\hat{s}} - k = 0.$$

We have then $l_2(\hat{s}) = 1$, $l_2(1) < 1$ and

$$l_2'(s) = -\frac{2}{\phi^2\psi}\left(\frac{\mu s}{\kappa+s} - k\right)\frac{\mu\kappa}{(\kappa+s)^2} < 0, \quad s > \hat{s},$$

and the reversed inequality for $0 < s < \hat{s}$. Thus, $l_2(s)$ is a strictly decreasing function for $\hat{s} < s < 1$ and strictly increasing for $0 < s < \hat{s}$.

We parameterize the $s$-nullcline as $\Lambda_1(s)$. It is implicitly given as

$$0 = \alpha\psi(1-\Lambda_1)^3(1-s) - \beta\frac{\Lambda_1 s}{\kappa+s} + 2s\left(\mu\frac{\Lambda_1 s}{\kappa+s} - k\Lambda_1 - \phi\sqrt{\psi}\sqrt{1-\Lambda_1}\Lambda_1\right).$$

Instead of calculating the equilibria as intersections of $\Lambda_1(s)$ and $l_2(s)$ directly, we note that in these points the last term of the last expression vanishes. Hence, equilibria are those points $(s^*, l^*) = (s, l)$ that lie on $l_2(s)$ and satisfy

$$0 = \alpha\psi(1-l)^3(1-s) - \beta l\frac{s}{\kappa+s}. \tag{29}$$

In other words, for every $s$ they can be found as the root of cubic polynomials. More specifically they can be determined as the intersections of the cubic function

$$\chi_1(l) = (1-l)^3$$

with the straight lines

$$\chi_2(l) = \frac{\beta s}{\alpha\psi(1-s)(\kappa+s)}l.$$

For every choice of $s$ in $[0, 1)$ and all model parameters fixed, this intersection is unique. Thus, there runs only one such curve, denoted by $l_1(s)$ in $I$. It is continuous and strictly decreasing with $l_1(0) = 1$. We find directly from (26) or by taking the limit for $s \to 1$ that $l_1(1) = 0$. See also Figure 4 to support these geometrical arguments.

By the intermediate value theorem, it follows that there exists exactly one nontrivial equilibrium $(\tilde{s}, \tilde{l})$ with $\tilde{s} < \hat{s}$, as an intersection point of the strictly decreasing function $l_1(s)$ with the strictly increasing function $l_2(s)$. We note that in this equilibrium the substrate concentration is too small to sustain biofilm growth, even in the absence of detachment. Thus we expect this equilibrium to be unstable.

Moreover, by the intermediate value theorem, it follows, that $l_1(s)$ and $l_2(s)$ have at least one intersection in a nontrivial equilibrium point $(s^*, l^*)$ with $s^* > \hat{s}$ and $l^* = l_1(s^*) = l_2(s^*)$ if

$$\left(\frac{\mu}{\kappa+1} - k\right)^2 > \phi^2\psi.$$

Recall that under this condition, the trivial equilibrium is unstable. On the other hand, since both $l_1(s)$ and $l_2(s)$ are monotonously decreasing and because $l_2(\hat{s}) > l_1(\hat{s})$, the particular form of (28) implies that for large enough values of $\phi^2\psi$ no equilibrium exists besides the then asymptotically stable trivial one.

It is difficult to calculate the values $s^*$ and $l^*$ explicitly in closed form. Therefore, we resort to numerical computations to investigate the existence and stability of the

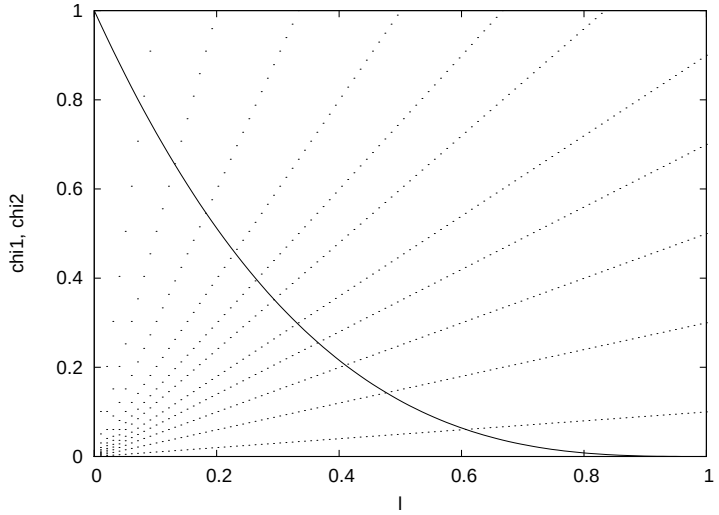


FIGURE 4. Functions $\chi_1(l) = (1-l)^3$ (solid line) and $\chi_2(l) = \frac{\beta s}{\alpha\psi(1-s)(\kappa+s)} l$ (dotted lines) for several choices of $s$. The slopes of the lines $\chi_2$ increase as $s$ increases. The intersections of these curves mark the points $(s, l_1(s))$.

TABLE 1. Model parameters used in simulations studies

| parameter | symbol | value | unit | reference |
|---|---|---|---|---|
| bulk substrate concentration | $S_\infty$ | 30 | $\mathrm{gm}^{-3}$ | [36] |
| biomass density | $X_\infty$ | 10000 | $\mathrm{gm}^{-3}$ | [36] |
| maximum growth rate | $\mu$ | 6 | $\mathrm{d}^{-1}$ | [36] |
| half saturation concentration | $K$ | 4 | $\mathrm{gm}^{-3}$ | [36] |
| cell death rate | $k$ | 0.4 | $\mathrm{d}^{-1}$ | [36] |
| yield coefficient | $Y$ | 0.63 | - | [36] |
| bulk viscosity | $\eta$ | 86.6 | $\mathrm{Ndm}^{-2}$ | [13] |
| bulk density | $\rho$ | $1 \cdot 10^6$ | $\mathrm{gm}^{-3}$ | [13] |
| reactor height | $H$ | 0.001 | m | assumed |
| reactor length | $L$ | 0.01 | m | assumed |
| compounded | $\alpha$ | $1.203 \cdot 10^{-8}$ | $m^3N^{-1}d^{-1}$ | calculated |
| compounded | $\beta$ | 1587.3 | $\mathrm{d}^{-1}$ | calculated |
| compounded | $\kappa$ | 0.133 | - | calculated |

non-trivial equilibria. To this end, we compute $l_1(s)$ for $s \in (0,1)$ numerically with Newton's method as solution to

$$(1-l)^3 - \frac{\beta s}{\alpha\psi(1-s)(\kappa+s)} l = 0$$

and we locate the nontrivial equilibria as intersections of $l_1(s)$ and $l_2(s)$. The stability of these equilibria is then determined from the Jacobian, given in the Appendix as (31), in the usual manner by determining its trace and determinant, or equivalently its eigenvalues.

We do not aim for a complete exploration of the twelve-dimensional parameter space, but focus on the effect of the parameters of the detachment model, i.e. the detachment coefficient $\delta$ and the hydrodynamic condition in the reactor. The model parameters used are summarized in Table 1. These values are chosen from a typical range of parameters, as documented in the biofilm literature, such as Benchmark Problem 1 in [36]. The compounded parameters $\beta$ and $\kappa$ are computed from these. Similarly, the compounded parameter $\alpha$ is fixed from standard parameters for water as the bulk liquid and a small microfluidic flow chamber. The parameters $\phi$ and $\psi$ are varied. From (17) we obtain the average flow velocity in an empty channel (with $l = 0$) as $u = \frac{1}{12}\psi H^2/\eta$. Thus the reactor Reynolds number is directly proportional to the pressure gradient $\psi$,

$$Re = \frac{1}{12}\frac{\rho}{\eta^2}H^3\psi.$$

For the parameters in Table 1 we compute the value for $\psi$ driving a flow with $Re = 1$ as $\psi|_{Re=1} = 6.71 \cdot 10^{20} Nm^{-3}$. This is well in the laminar regime for which our flow approximation is valid.

We vary $\psi$ such that it covers the range of reactor Reynolds numbers $Re = 10^{-8} \sim 10^{-4}$ and test several values of the detachment coefficient $\phi$ for each of them. In Figure 5 we plot for selected choices of $\psi$ and $\phi$ the functions $l_1(s)$ and $l_2(s)$ and report the equilibria and their stability. These are representative snapshots of the overall picture. From our computations we observe three possible distinct cases, the transitions between which are continuous:

(a) For large values of $\phi^2\psi$ the functions $l_1(s)$ and $l_2(s)$ do not intersect for $s > \hat{s}$. In this case, $l_2(s) > l_1(s)$ for all $s \in [\hat{s}, 1]$. With the arguments presented above the trivial equilibrium is stable under these conditions. The combination of large flow velocities, and hence shear forces, and high detachment rate coefficients does not allow a biofilm to establish itself.
(b) For intermediate values of $\phi^2\psi$ we find two non-trivial equilibria, $(s_1^*, l_1^*)$ and $(s_2^*, l_2^*)$, with $\hat{s} < s_1^* < s_2^*$ and $l_1^* > l_2^*$. The equilibrium $(s_1^*, l_1^*)$ is a stable node, the equilibrium $(s_2^*, l_2^*)$ is a saddle. Since in these cases $l_2(1) > 0$, the trivial equilibrium is asymptotically stable.
(c) For small enough values

$$\phi^2\psi < \left(\frac{\mu}{\kappa + 1} - k\right)^2$$

there is only one non-trivial equilibrium $(s^*, l^*)$ with $s^* > \hat{s}$, which is a stable node. The smaller $\phi^2\psi$ the smaller will be $s^*$ and the larger will be $l^*$. We observe $s^*$ to be substantially smaller than the maximum value 1, often close to $\hat{s}$, and the biofilm thickness $l^*$ can be close to the maximum value 1. The low values of $s^*$ indicate that the equilibrium is reached because of a substrate depletion. Under these conditions, the trivial equilibrium is unstable.

In all cases (a), (b), (c) we confirm the non-trivial equilibriums $(\tilde{s}, \tilde{l})$ with $0 < \tilde{s} < \hat{s}$ to be unstable.

The stable nodes according to (b),(c) are found to correspond to thick biofilms, indeed close to complete clogging of the flow channel, $l^* \approx 1$. The bulk substrate concentration is very small, close to $\hat{s}$, indicating growth limitations. Note that these substrate limitations have two causes: the thick biofilm implies high substrate demand, as well as a small flow rate, i.e. low supply. The unstable saddle according

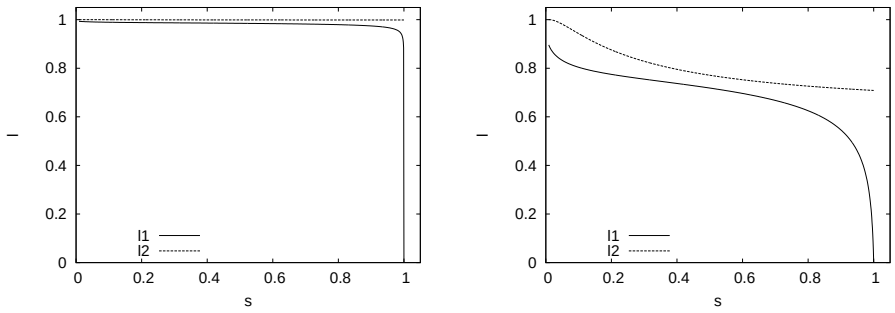


(i) $Re = 10^{-4}, \phi = 5 \cdot 10^{-7}$ (ii)$Re = 10^{-8}, \phi = 3.5 \cdot 10^{-6}$

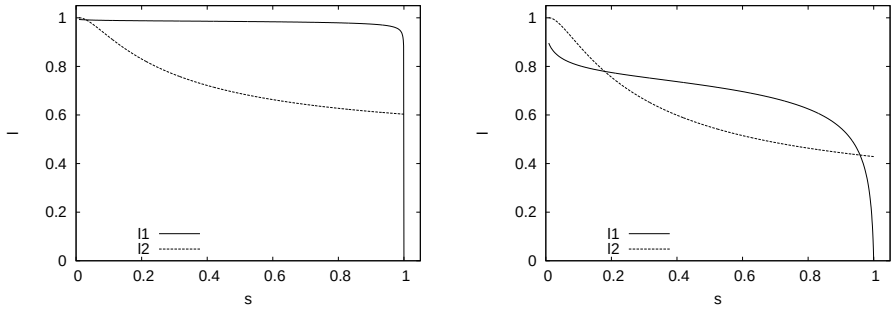


(iii) $Re = 10^{-4}, \phi = 3 \cdot 10^{-8}$ (iv)$Re = 10^{-8}, \phi = 2.5 \cdot 10^{-6}$

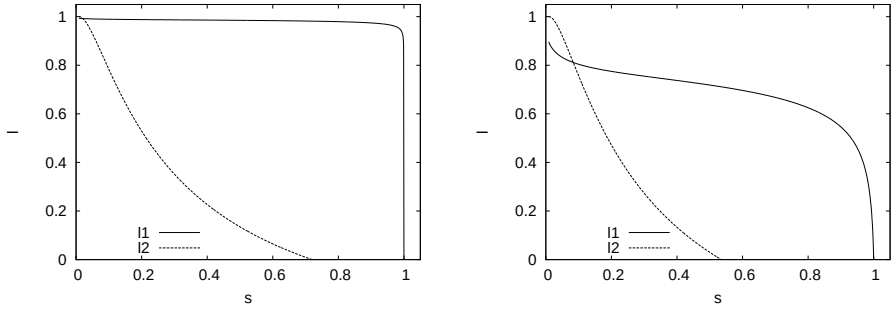


(v) $Re = 10^{-4}, \phi = 1.8 \cdot 10^{-8}$ (vi)$Re = 10^{-8}, \phi = 1.7 \cdot 10^{-6}$

FIGURE 5. $l_1(s)$ and $l_2(s)$ in $[\hat{s}, 1] \times [0, 1]$. The intersections of these curves are the equilibria: (i) no nontrivial equilibrium, (ii) no nontrivial equilibrium, (iii) stable node at $(0.030032, 0.99181)$, saddle at $(0.99969, 0.60338)$, (iv) stable node at $(0.17868, 0.780164)$, saddle at $(0.95743, 0.43523)$, (v) stable node at $(0.021739, 0.99104)$, (vi) stable node at $(0.08398, 0.81010)$. In all cases an additional unstable equilibrium is found in $I$ for a $0 < \tilde{s} < \hat{s}$ (not shown). The trivial equilibrium at $(1, 0)$ is stable for (i),(ii),(v),(vi), unstable for (iii),(iv).

to (b), on the other hand is attained for $s_2^* \approx 1$ i.e. it is not growth limited but hydrodynamically limited.

For a fixed flow regime, expressed in terms of $\psi$, the detachment parameter $\phi$ plays the deciding role for the qualitative long term behavior. Comparing our

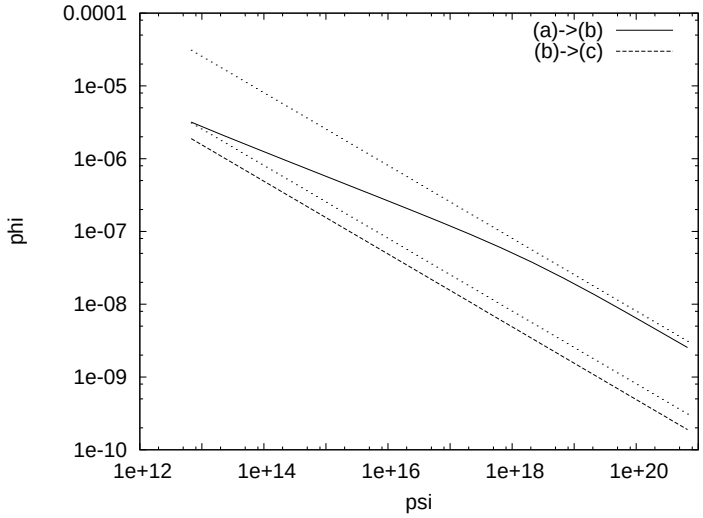


FIGURE 6. Computed critical value $\phi_{critical,(a)\to(b)}$ for the transition from state (a) with no non-trivial equilibrium in $(\hat{s},1)\times(0,1)$ to the the state (b) with a stable and an unstable non-trivial equilibrium, as a function of pressure gradient $\psi$ (solid curve); $\psi$ covers hydrodynamic reactor conditions corresponding to $10^{-8} < Re < 10$. The two dotted curves are upper and lower estimates on $\phi_{critical,(a)\to(b)}$, parameterized as $\phi = 8/\sqrt{\psi}$ and $\phi = 80/\sqrt{\psi}$. Also plotted is the analytically computed value $\phi_{critical,(b)->(c)} = \left(\frac{\mu}{1+\kappa} - k\right)/\sqrt{\psi} = 4.9/\sqrt{\psi}$.

simulation results we find that the critical values for $\phi$ at which the transitions from state (a) to (b) or from (b) to (c) occur increases with decreasing reactor Reynolds number. For the transition from (b) to (c), this can be calculated easily from (27) as

$$\phi_{critical,(b)\to(c)} = \frac{1}{\sqrt{\psi}}\left(\frac{\mu}{\kappa+1} - k\right),$$

i.e. a two order of magnitude change in $\psi$ induces a one order of magnitude change in $\phi_{critical,(b)\to(c)}$. A similar qualitative relation is confirmed computationally for the other transition

$$\phi_{critical,(a)\to(b)} \sim \frac{1}{\sqrt{\psi}},$$

plotted in Figure 6.

We conclude that the detachment coefficient $\delta$, whence $\phi$, that is required to obtain a stable biofilm that maintains an unclogged flow path depends on the reactor shear rate. In our modeling framework, $\delta$ was considered a parameter that describes material properties of the biofilm, independent of the hydrodynamic conditions. Experimental studies, however, suggest that the material properties of the biofilm are not only strain specific but also depend on the conditions under which the biofilm was grown, including bulk substrate supply and, more importantly in our context, the hydrodynamic conditions in the reactor [9, 22, 30, 32]. More specifically, biofilms grown under higher reactor shear-rates are mechanically stronger biofilms. In the

framework of our model, this would indeed translate into the detachment coefficient $\delta$, whence $\phi$, to be smaller for larger $\psi$. A quantitative relationship between detachment coefficient and the bulk flow conditions under which the biofilm was grown is not known in the literature. In order to include this in the model one must keep in mind that it is the growth history rather than the current conditions that must be considered. This could potentially be modeled by a nonlocal retardation term, which however will increase the mathematical complexity of the model drastically.

Note that the interval $I$ is not positively invariant. To see this, substitute $l = 1$ into the equation for $l$ in (26) and find $dl/dt > 0$ for $s > \hat{s}$. Thus the existence of asymptotically stable equilibria in $I$ does not necessarily guarantee that the solutions converge to steady state. Solutions for which eventually $l > 1$ loose their physical meaning. They represent that the channel clogs and mark the breakdown of the model. Whether this happens or whether the solution converges to a stable equilibrium depends on the initial data. In experimental studies, often the biofilm is initially grown under certain conditions and then placed either in a different environment or reactor conditions such as bulk substrate concentrations and reactor shear rate are instantaneously changed. In such a set-up the equilibria and their stability change instantaneously, because the parameters change. Hence, such abrupt changes can change the dynamics of the biofilm system.

## 6. **Conclusion.**

Traditional one-dimensional mathematical models of biofilms for realistic multi-species systems are described by a free boundary value problem for a mixed hyperbolic-parabolic system. This makes them very difficult to access for qualitative mathematical analysis, and what is known about them has been primarily derived in numerous quantitative computer simulation case studies. For simpler single species systems, on the other hand, we could rewrite the free boundary value problem as an ordinary differential equation, which allows us to study it with elementary techniques. Using this approach we investigated the role of the choice of the particular biofilm detachment model and the role of the hydrodynamic regime for the long term behavior of the model.

The detachment rate expressions commonly used in the literature do not account for the fact that the shear rate acting on the biofilm contributes to biomass loss. If at all, flow effects are only accounted for by adjusting the detachment coefficients for reactor hydrodynamics but it is neglected that biofilm growth in return can alter the hydrodynamics. We studied here two detachment rate expressions that explicitly account for this effect. One, denoted by us as $d_3$, has been been proposed previously in the literature by fitting against experimental data. The other one, denoted by $d_4$, was proposed here as a phenomenological criterion that assumes the detachment rate to be proportional to both, biofilm thickness and the local shear rate. We find that the choice of the detachment rate functions can affect the equilibria and their stability. For example, the stability of the washout equilibrium depends on the bulk flow hydrodynamics if detachment rate $d_3$ is used, but it is independent of the flow conditions if detachment rate $d_4$ is used instead. From this view point, the detachment model $d_3$ can be understood as a hydrodynamic generalization of the first order detachment model (constant detachment coefficient), while $d_4$ can be understood as a hydrodynamic generalization of the more frequently used second order detachment model (detachment rate scales with biofilm thickness).

Also the hydrodynamic regime can have a major impact on the qualitative long term behavior of the model solutions, in particular they can affect whether a biofilm

can establish itself, and if so whether or not it will eventually clog the channel or leave an open flow path. Commonly, the reactor scale Reynolds number is used to characterize the flow conditions in a biofilm reactor. By analyzing three types of flow scenarios for the two shear rate dependent detachment models, namely (i) Couette flow that mimics narrow gap rotating annulus biofilm reactors, (ii) pressure drop driven Poiseuille flow that for example mimics trickling filters or porous media biofilm reactors, and (iii) flow rate driven Poiseuille flow that mimics microfluidics chambers, we find that this is not a sufficient criterion to predict the effect of hydrodynamics on the biofilm. For example, while flow mechanisms (i) and (iii) guarantee an open flow path, flow mechanism (ii) can lead to clogging of the flow channel for the same reactor scale Reynolds number.

In the case of detachment rate functions that do not explicitly depend on reactor hydrodynamics, it depends only on the detachment rate coefficient whether the channel clogs. The model is not prevented from predicting and reaching an unphysical stable equilibrium.

Our analysis was originally carried out for a single-species/single-substrate biofilm model, for which biofilm growth does not affect the bulk substrate concentration. Using comparison theorems, we were able to partially apply the qualitative results to more complicated systems, such as multi-species/multi-substrate biofilm systems or biofilm models that are embedded in a reactor mass balance for a dissolved substrate that is degraded by biofilm activity. In particular we construct in both cases a single-species/single-substrate biofilm model which gives us an upper bound on the biofilm thickness of the more involved system. If this upper estimates predicts that the system will not clog entirely but a flow path will be maintained, then this applies also to the underlying more complex model. If the upper estimate predicts washout, also the underlying more complex model will predict washout.

As discussed above, in contrast to Couette flow or flow rate driven Poiseuille flow, a pressure gradient driven Poiseuille flow does not necessarily guarantee that a flow path will be maintained and that the channel does not clog. This becomes in particular obvious in a reactor setup where the growth of the biofilm leads to a decrease of the bulk substrate concentration due to consumption. Under these circumstances, an increasing pressure gradient applied to the flow channel increases on the one hand the flow rate and therefore substrate supply and washout, as well as the detachment forces. On the other hand, the increased substrate supply leads to accelerated growth which obstructs the flow and thus reduces the flow rate. Growth, bulk flow, and detachment interact intricately. The qualitative longterm behavior and its stability in this setup depends sensitively both on reactor flow conditions and on the material properties of the biofilm.

In summary, in biofilm modeling, the choice of the detachment rate function used and the reactor flow conditions can drastically determine the longterm behavior of the biofilm. They affect at least the biofilm thickness predicted, but can even affect qualitative persistence predictions. This seems to indicate that biofilm detachment studies, both theoretical and experimental, must be seen in the context of the particular reactor and flow regime.

**Acknowledgments.** This study was supported in parts by MPRIME (a Network of Centers of Excellence) through the seed project *Mathematical Models of Biofilm Deformation and Detachment*. FA also acknowledges the support received trhough

a graduate scholarship from the Higher Education Commission of Pakistan. HJE acknowledges the support received from the Canada Research Chair program.

## REFERENCES


[1] F. Abbas and H. J. Eberl, *Analytical substrate flux approximation for the Monod boundary value problem*, Appl. Math. Comp., **218** (2011), 1484–1494.

[2] J. P. Boltz, E. Morgenroth, D. Brockmann, C. Bott, W. J. Gellner and P. A. Vanrolleghem, *Critical components of biofilm models for engineering practise*, in "Proceedings Conf. Water Env. Fed. Tech. Exh. Conf. WEFTEC 2010," (2010), 1072–1098.

[3] J. D. Bryers, *Biofilm formation and chemostat dynamics: Pure and mixed culture considerations*, Biotech. Bioeng., **26** (1984), 948–958.

[4] S. Carl and S. Heikkilä, "Nonlinear Differential Equations in Ordered Spaces," Chapman & Hall/CRC Monographs and Surveys in Pure and Applied Mathematics, **111**, Chapman & Hall/CRC, Boca Raton, FL, 2000.

[5] M. A. S. Chaudhry and S. A. Beg, *A review on the mathematical modeling of biofilm processes: Advances in fundamentals of biofilm modeling*, Chem. Eng. Technol., **21** (1998), 701–710.

[6] B. M. Chen-Charpentier and H. V. Kojouharov, *Numerical simulation of dual-species biofilms in porous media*, Appl. Num. Math., **47** (2003), 377–389.

[7] B. M. Chen-Charpentier and H. V. Kojouharov, *Mathematical modeling of bioremediation of trichloroenthylene in aquifers*, Comp. Math. Appls., **56** (2008), 645–656.

[8] N. Derlon, A. Massé, R. Escudié, N. Bernet and E. Paul, *Stratification in the cohesion of biofilms grown under various environmental conditions*, Water Research, **42** (2008), 2102–2110.

[9] B. C. Dunsmore, A. Jacobsen, L. Hall-Stoodley, C. J. Bass, H. M. Lappin-Scott and P. Stoodley, *The influence of fluid shear on the structure and material properties of sulphate-reducing bacterial biofilms*, J. Ind. Microbiol. Biotech., **29** (2002), 347–353.

[10] H. Horn, T. R. Neu and M. Wulkow, *Modelling the structure and function of extracellular polymeric substances in biofilms with new numerical techniques*, Wat. Sci. Tech., **43** (2001), 121–127.

[11] J. C. Kissel, P. L. McCarty and R. L. Street, *Numerical simulation of mixed-culture biofilm*, ASCE J. Env. Eng., **110** (1984), 393–411.

[12] I. Klapper and B. Szomolay, *An exclusion principle and the importance of mobility for a class of biofilm models*, Bull. Math. Biol., **73** (2011), 2213–2230.

[13] H. Kuchling, "Physik," $18^{th}$ edition, VEB Fachbuchverlag Leipzig, 1987.

[14] Z. Lewandowski and H. Beyenal, "Fundamentals of Biofilm Research," CRC Press, 2007.

[15] A. Masic, J. Bengtsson and M. Christensson, *Measuring and modeling the oxygen profile in a nitrifying moving bed biofilm reactor*, Math. Biosc., **227** (2010), 1–11.

[16] A. Masic and H. J. Eberl, *Persistence in a single species CSTR model with suspended flocs and wall attached biofilms*, Bull. Math. Biol., to appear.

[17] E. Morgenroth, *Detachment: An often-overlooked phenomenon in biofilm research and modelling*, in "Biofilms in Wastewater Treatment" (eds. S. Wuertz et al), IWA Publishing, (2003), 246–290.

[18] N. Muhammad and H. J. Eberl, *Open MP parallelization of a Mickens time-integration scheme for a mixed-culture biofilm model and its performance on multi-core and multi-processor computers*, LNCS, **5976** (2010), 180–195.

[19] N. Muhammad and H. J. Eberl, *Model parameter uncertainties in a dual-species biofilm competition model affect ecological output parameters much stronger than morphological ones*, Math. Biosc., **233** (2011), 1–18.

[20] B. R. Munson, D. F. Young and T. H. Okiishi, "Fundamentals of Fluid Mechanics," John Wiley & Sons, 1990.

[21] N. C. Overgaard, *Application of variational inequalities to the moving-boundary problem in a fluid model for biofilm growth*, Nonlin. Analysis, **70** (2009), 3658–3664.

[22] E. Paramonova, O. J. Kalmykowa, H. C. van der Mei, H. J. Busscher and P. K. Sharma, *Impact of hydrodynamics on oral biofilm strength*, J. Dent. Res., **88** (2009), 922–926.

[23] B. M. Peyton and W. G. Characklis, *A statistical analysis of the effect of substrate utilization and shear stress on the kinetics of biofilm detachment*, Biotech. Bioeng., **41** (1982), 728–735.

[24] L. A. Pritchett and J. D. Dockery, *Steady state solutions of a one-dimensional biofilm*, Math. Comp. Model., **33** (2001), 255–263.

[25] B. E. Rittmann and P. L. McCarty, *Model of steady state biofilm kinetics*, Biotech. Bioeng., **22** (1980), 2343–2357.

[26] B. E. Rittmann, *The effect of shear stress on biofilm loss rate*, Biotech. Bioeng., **24** (1982), 501–506.

[27] B. E. Rittmann, A. O. Schwarz, H. J. Eberl, E. Morgenroth, J. Perez, M. C. M. van Loosdrecht and O. Wanner, *Results from the multi-species benchmark problem (BM3) using one-dimensional models*, Wat. Sci. & Tech., **49** (2004), 163–168.

[28] B. E. Rittmann, D. Stilwell and A. Ohashi, *The transient-state, multiple-species biofilm model for biofiltration processes*, Water Research, **36** (2002), 2342–2356.

[29] A. Rochex, A. Massé, R. Escudié, J. J. Godon and N. Bernet, *Influence of abrasion on biofilm detachment: Evidence for stratification of the biofilm*, J. Ind. Microbiol. Biotech., **36** (2009), 467–470.

[30] P. Stoodley, R. Cargo, C. J. Rupp, S. Wilson and I. Klapper, *Biofilm material properties as related to shear-induced deformation and detachment phenomena*, J. Ind. Microbiol. Biotech., **29** (2002), 361–367.

[31] B. Szomolay, *Analysis of a moving boundary value problem arising in biofilm modelling*, Math. Meth. Appl. Sci., **31** (2008), 1835–1859.

[32] U. Telgmann, H. Horn and E. Morgenroth, *Influence of growth history on sloughing and erosion from biofilms*, Water Research, **38** (2004), 3671–3684.

[33] L. Tijhuis, M. C. M. van Loosdrecht and J. J. Heijnen, *Dynamics of biofilm detachment in biofilm airlift suspension reactors*, Biotech. Bioeng., **45** (1995), 481–487.

[34] M. M. Trulear and W. G. Characklis, *Dynamics of biofilm processes*, J. Water Pollut. Control Fed., **54** (1982), 1288–1301.

[35] W. Walter, "Gewöhnliche Differentialgleichungen," $7^{th}$ edition, Springer-Verlag, 2000.

[36] O. Wanner, H. Eberl, E. Morgenroth, D. Noguera, C. Picioreanu, B. Rittmann and M. van Loosdrecht, "Mathematical Modeling of Biofilms," IWA Publishing, 2006.

[37] O. Wanner and W. Gujer, *A multispecies biofilm model*, Biotech. Bioeng., **28** (1986), 314–328.

**Appendix** A. **Jacobian of the model of Section 5.2.** The Jacobian of the full system (22) is obtained as

$$F'(S,\lambda)=\begin{pmatrix} \frac{-1}{H-2\lambda}\left(\frac{Q(\lambda)}{L}+\frac{X_\infty}{Y}j_S(\lambda,S)\right) & \frac{2}{(H-2\lambda)^2}\left[\frac{Q(\lambda)}{L}(S_\infty-S)\right. \\ +\frac{2}{H-2\lambda}\left[\frac{d\lambda}{dt}+2Sj_S(\lambda,S)\right] & \left.-\frac{X_\infty}{Y}j(\lambda,S)+2S\frac{d\lambda}{dt}\right] \\ & +\frac{1}{H-2\lambda}\left[\frac{Q'(\lambda)}{L}(S_\infty-S)-\frac{X_\infty}{Y}j_\lambda(\lambda,S)\right] \\ & +\frac{2S}{H-2\lambda}\left[j_\lambda(\lambda,S)-k-d(\lambda)-d'(\lambda)\lambda\right] \\ \\ j_S(\lambda,S) & j_\lambda(\lambda,S)-k-d(\lambda)-d'(\lambda)\lambda \end{pmatrix}. \tag{30}$$

Note that the first term of the entry in position (1,2) vanishes if the Jacobian is evaluated in an equilibrium. Moreover, in the trival equilibrium $(s^*,\lambda^*)=(S_\infty,0)$ we obtain with $j_s(0,S_\infty)=0$ the Jacobian in the form (24).

For the nontrivial equilibria $(s^*,l^*)$ in the special case of (26) the Jacobian simplifies to

$$F'(s^*, l^*) = \begin{pmatrix} -\alpha\psi(1-l^*)^2 & -2\alpha\psi(1-l^*)(1-s^*) \\ -(\beta - 2\mu s^*)\frac{l^*}{1-l^*}\frac{\kappa}{(\kappa+s^*)^2} & -\beta\frac{s^*}{\kappa+s^*}\frac{1}{(1-l^*)^2} + \frac{2s^*}{1-l^*}\frac{\phi\sqrt{\psi}l^*}{2\sqrt{1-l^*}} \\ \mu l\frac{\kappa}{(\kappa+s^*)^2} & \frac{\phi\sqrt{\psi}l^*}{2\sqrt{1-l^*}} \end{pmatrix}. \tag{31}$$

Received May 29, 2011; Accepted August 16, 2011.

*E-mail address*: fabbas@uoguelph.ca
*E-mail address*: rsudarsa@uoguelph.ca
*E-mail address*: heberl@uoguelph.ca